Article

Not peer-reviewed version

A Metabolomic Investigation of the Effects of Corrosion Products of Galvanic Anodes on the Metabolome of Magallana gigas (Formerly Crassostrea gigas)

Nathalie Imbert-Auvray , Denis Fichet , Pierre-Edouard Bodet , Pascaline Ory , René Sabot , Philippe Refait * , Marianne Graber *

Posted Date: 6 June 2023

doi: 10.20944/preprints202306.0368.v1

Keywords: metabolomics; oysters; corrosion products modelling; sacrificial galvanic anode; zinc; aluminum; biological effects; bioaccumulation.

Article

A Metabolomic Investigation of the Effects of Corrosion Products of Galvanic Anodes on the Metabolome of *Magallana gigas* (Formerly *Crassostrea gigas*)

Nathalie Imbert Auvray [1], Denis Fichet [1], Pierre-Edouard Bodet [1], Pascaline Ory [1], René Sabot [2], Philippe Refait [2,*] and Marianne Graber [1,*]

[1] UMR 7266 LIENSs, CNRS-La Rochelle Université, 2 Rue Olympe de Gouges, 17000 La Rochelle, France; nathalie.imbert@univ-lr.fr (N.I.A.); denis.fichet@univ-lr.fr (D.F.); pierreedouard.bodet@univ-lr.fr (P.-E.B.); pascaline.ory01@univ-lr.fr (P.O.); marianne.graber@univ-lr.fr (M.G.)

[2] UMR CNRS 7356 LaSIE, CNRS-La Rochelle Université, Avenue Michel Crépeau, 17042 La Rochelle, France; rene.sabot@univ-lr.fr

* Correspondence: philippe.refait@univ-lr.fr (P.R.); marianne.graber@univ-lr.fr (M.G.)

Abstract: Cathodic protection is widely used to protect metal structures from corrosion and is commonly applied on marine structures in seaports using sacrificial galvanic anodes. These anodes, either in Zinc, or preferentially nowadays in Al-Zn-In alloys, are expected to corrode instead of the metal to be protected. This leads to the release of specific dissolved species, Zn^{2+}, Al^{3+}, In^{3+} and solid phases like $Al(OH)_3$. Few studies were conducted on the effects of anodes on marine organisms and concluded that further detailed investigations are needed in controlled environments. We therefore propose an experimental approach to evaluate the effects of Zn and Al-Zn-In anodes on oysters stabulated in tanks, under conditions approaching those used in the ports. We chose a non-targeted metabolomic approach, using UHPLC coupled to HRMS, to study the effects on the entire metabolome, without any *a priori*. A modelling study of the chemical species, corresponding to the degradation products of the anodes, likely to be present near the exposed oysters, was also included. We identified 16 and 2 metabolites modulated by Zn- and Al-Zn-In-anodes respectively, involved in biological functions, such as energy metabolism, osmoregulation, oxidative stress, lipid, nucleotide nucleoside and amino acid metabolisms, defense and signaling pathways.

Keywords: metabolomics; oysters; corrosion products modelling; sacrificial galvanic anode; zinc; aluminum; biological effects; bioaccumulation

1. Introduction

Cathodic protection (CP) is widely used to protect metal structures from corrosion in marine applications, e.g., ship hulls and propellers, seaports steel sheet pilings, offshore oil platforms or marine renewable energy devices, and so on. CP is commonly applied on marine metal structures using galvanic anodes, a concept first proposed and successfully implemented by Davy in 1824 [1]. Zinc has been a common material for galvanic anodes due to its high efficiency but nowadays aluminum-based alloys, and in particular Al-Zn-In alloys, are considered to offer the best performance in seawater [2–4].

The protection of seaports structures may require the use of hundreds of tons of galvanic anodes, which are expected to corrode instead of the metal, mainly carbon steel in this case, constituting the structure to be protected. This corrosion process then leads to the formation of dissolved species, e.g., Zn^{2+}, In^{3+}, and Al^{3+}, and solid phases, e.g., $Al(OH)_3$, which are released in the seaport water. The need to assess the environmental impact of galvanic anodes was then expressed and a few studies were

 doi:10.20944/preprints202306.0368.v1

devoted to this problem [5–8]. Very recently, a study was set up over two years (2020 and 2021) to observe whether Al-Zn-In-sacrificial anodes had an impact on the health status of the black scallop *Mimachlamys varia* in a port environment (commercial port and marina of La Rochelle, France), using a multi-biomarker approach [7,9]. The conclusion was that port activities, as well as meteorological conditions, influenced the biomarker results too significantly and masked the potential effects of these anodes. It was finally suggested that it would therefore be interesting to carry out a similar study in a controlled environment to be free from the influence of port activities and conditions [7]. In 2022, the toxicity of an Al-Zn-In-based galvanic anode on the Pacific oyster, *Magallana gigas* was studied in controlled conditions. Oysters were exposed for about three months to different anode degradation products concentrations, obtained with an electrochemical experimental device simulating the dissolution of a galvanic anode. Different biomarkers of the immune system, reproductive parameters and the metabolic state of the oysters were studied and bioaccumulation of metals coming from the anodes was measured. Analyses shown that oyster bioaccumulated Al and Zn and demonstrated some biological effects at the highest concentrations, far above those found in the environment, linked with a possible impairment of immune system and oxidant stress defense at the end of exposure [8]. Further investigations are needed to analyze other potential effects of anodes on marine organisms and to compare Zn- and Al-Zn-In-anodes in conditions approaching exposure levels in port environments.

We therefore propose here an experimental approach in a controlled environment, to evaluate on oysters stabulated in tanks, the comparative effects of Zn- and Al-Zn-In-anodes, operating under similar conditions to those used in the ports of La Rochelle. In general, Zn-based and Al-Zn-In-based sacrificial anodes contain various trace elements, e.g., Fe or Cu, but the current study is focused on the elements specific to the anodes, i.e., Al, Zn and In. We have included in the present study a modelling of the chemical species corresponding to the degradation products of the anodes, likely to be present in the vicinity of the exposed oysters. Moreover, we chose a non-targeted metabolomic approach using ultra-high performance liquid chromatography coupled to high resolution mass spectrometry (UHPLC-HRMS), to study the effects of these anodes on the entire metabolome of oysters with a high level of sensitivity, without any *a priori*.

2. Materials and Methods

2.1. Experimental Organisms

The experiment was carried out in June 2021, in mesocosm located in a salt marsh in laboratory LIENSs experimental facilities (46°12’13.835” N; 1°11’43.572” O).

Eighteen-month-old Pacific oysters, *Magallana gigas*, (averaged total flesh weight = 22.9 ± 5.9 g, $n = 100$) were purchased from a local shellfish farm France Naissain®. These triploid oysters originated from the same resource. After eight days acclimation, oysters were randomly divided into three groups and held in tank (200 L) receiving a constant flow of external water (**Figure 1**). Each tank was continuously aerated and totally renewed each day (200 L per day) with seawater collected from our experimentation salt marsh. Before using, seawater was first decanted in a 16,000 L tank located outside of the lab. Oysters were maintained and fed throughout the experiment (16 days) by the planktonic communities present in natural sea water of the oyster ponds. The tanks were checked every day to remove the potential dead oysters (temperature 22 ± 2 °C; salinity 37 ± 1 ‰).

Preprints (www.preprints.org) | NOT PEER-REVIEWED | Posted: 6 June 2023 doi:10.20944/preprints202306.0368.v1

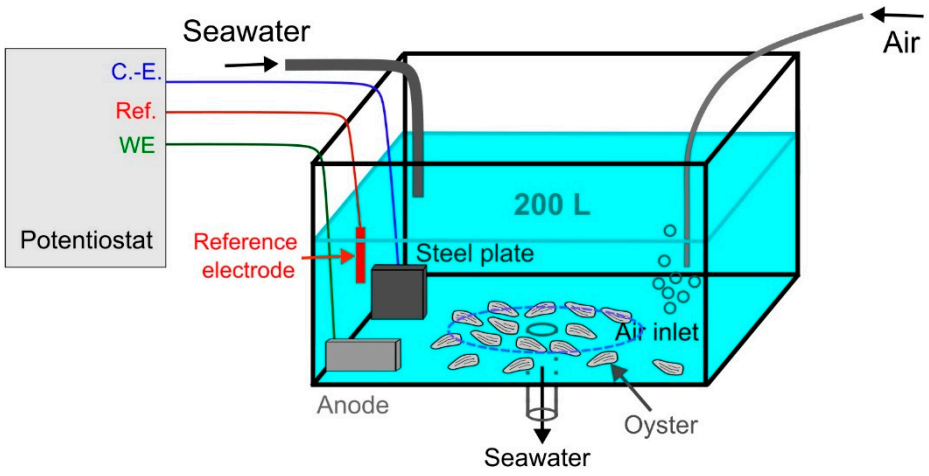

Figure 1. Schematic representation of the experimental setup consisting of potentiostat, galvanic anode, passive sampler and oysters exposed to the product of anode dissolution in an open-circuit tank. The LSNM-NP passive samplers were set among the oysters, inside the area demarcated by the dashed blue line (C.-E.: Counter–electrode; Ref.: reference electrode; WE: working electrode).

2.2. Experimental Setup

Two kinds of anodes have been tested as cathodic protection: an anode mainly composed of zinc called «Zn-anode» and an anode mainly composed of aluminum called «Al-Zn-In-anode» (see § 2.3). 33 oysters were placed on the bottom of each tank (**Figure 1**): a tank without cathodic protection (control), a tank equipped with the Zn-anode and a tank equipped with the Al-Zn-In anode. Oysters have been exposed for 16 days to the product of anodes dissolution.

Passive samplers (LSNM-NP for cationic metals / DGTÒ Research) were used to confirm the presence of dissolved metal in water. Four samplers were placed successively in each tank. Each sampler was exposed for four days.

2.3. Cathodic Protection

One of the main concerns for the present study was to estimate what could be the representative conditions prevailing in a seaport. Among the most important parameters defining realistic conditions is the ratio between the mass of galvanic anodes present inside the seaport perimeter and the volume of seawater enclosed in this perimeter. As an example, the commercial seaport of La Rochelle (Atlantic coast) was considered. The average volume of water present inside the seaport perimeter was estimated at 5.55×10^6 m^3 and the overall mass of Al-Zn-In anodes used for the cathodic protection of the steel structures is equal to 135×10^3 kg. These anodes used for the cathodic protection of the La Rochelle seaport steel structures contain a maximum Zn content of 3.0 wt.%, a specific requirement of the seaport managers. The amount of In for this kind of alloy is usually very low, i.e., about 0.02 wt.%, a composition that ensures an active dissolution of the Al matrix [2–4].

For these anodes, the specific elements released in the environment are then Al (~97 wt.%), Zn (3 wt.%) and In (~0.02 wt.%). It is expected that the anodes are entirely consumed after 20 years, which, assuming a constant dissolution rate, corresponds to the release of 17.9 kg per day of aluminum, 0.55 kg per day of zinc and 3.7 g per day of In, for an overall mass of 135×10^3 kg. Considering the overall volume of the commercial seaport of La Rochelle, this mass per day corresponds to Al^{3+}, Zn^{2+} and In^{3+} released concentrations of 3.23 µg/L per day, 0.1 µg/L per day, and 0.0007 µg/L per day, respectively.

The flow of released matter can be controlled in laboratory experiments via the control of the current flowing through the anode. In this study, a constant anodic current, I = 2 mA, was applied using a potentiostat/galvanostat BioLogic SP300 with a three-electrode setup. The working electrode

 doi:10.20944/preprints202306.0368.v1

(WE) was the galvanic anode, with a surface of 5 cm^2 for all experiments. A common Al-Zn-In anode was used, i.e., the Zn content was 5 wt. %. The counter-electrode (C.-E.) consisted of a large carbon steel plate (surface of 125 cm^2), which thus simulated the protected seaport structure. The reference electrode (Ref.) was an Ag/AgCl/seawater electrode, with a potential E_{ref} = +250 mV/SHE. The overall experimental setup is displayed in Figure 1.

The Al-Zn-In anode is mostly made of aluminum and it can be assumed as a first approximation that the current is mainly associated with the oxidation of Al. Thus, according to the following anodic reaction, when 1 Al^{3+} ion is produced, 3 electrons are involved:

$$Al \rightarrow Al^{3+} + 3e^- \quad (1)$$

Consequently, the anodic current value of 2 mA ensures the production of 16 mg per day of Al(III) species. Considering the volume of seawater present inside the tank used for the experiments, i.e., 200 L, this production corresponds to a released Al(III) concentration of 80 µg/L per day. This value is then 25 times higher than the value estimated above as representative of the conditions prevailing in the commercial seaport of La Rochelle. The same ratio applies for the In released concentration, which was then about 0.017 µg/L per day in our experimental conditions. The Zn amount of the anode used for the experiment was higher than the Zn amount of the anodes used in the seaport of La Rochelle, i.e., 5% vs 3%, so that the ratio was about 25 × 5/3 ~ 42, leading to a Zn released concentration of 4.2 µg/L per day in our experimental conditions.

As displayed in Figure 1, seawater flowed continuously through the tank so that the overall 200 L volume was entirely renewed after 24 hours. The three electrodes were set close to the seawater input, favoring the detachment of the loose white layer of corrosion products ($Al(OH)_3$ at temperatures below 70°C [10]) formed on the anode surface. On the other side of the tank, an air inlet ensured the aeration of the seawater. The studied oysters were placed at the bottom of the tank, around the seawater outlet. It must be noted that the designed laboratory experiment relates to an open system, i.e., the produced Al(III) species may not accumulate inside the tank, though the solid $Al(OH)_3$ particles may remain at the bottom of the tank together with the studied oysters. The same situation prevails in a seaport, which is not a closed system either.

Nowadays, it is generally admitted that Al-Zn-In anodes present the best performance in seawater. However, Zn anodes were widely used [2,3] and some remain in service. The experiment was then carried out as described above using a pure (99.9 wt.%) Zn galvanic anode instead of an Al-Zn-In anode. For a Zn anode, the anodic reaction involves two electrons per Zn^{2+} ions produced:

$$Zn \rightarrow Zn^{2+} + 2e^- \quad (2)$$

The same current, I = 2 mA, was applied to control the dissolution of Zn anodes so that 58 mg per day of Zn(II) species were produced, corresponding to a released Zn(II) concentration of 290 µg/L per day in the tank containing 200 L of seawater.

2.4. Chemical Modelling

The corrosion of galvanic anodes in seawater leads to the formation of solid phases. In principle, these compounds do not form an adherent protective layer, because the corrosion of the anode must take place so that CP remains efficient. Depending on the hydrodynamic conditions, solid phase particles are carried away from the anode. The solubility of the corrosion products then governs the maximum local (i.e., close to the solid phase particles) dissolved Al or Zn species concentration (dilution in the overall amount of seawater contained in the seaport of course leads to much lower concentrations). An estimate of this maximum local concentration was determined via a theoretical approach based on a chemical modelling carried out with the PHREEQC Interactive software [11] (version 3.5, 2019) using the PHREEQC Minteq V4 database, derived from MINTEQ A2 version 4 [12,13]. A simplified seawater composition was used for computations and only the main seawater elements were considered. The concentrations, based on the ASTM D1141 standard [14], were as follows (in mmol kg^{-1}): [Cl^-] = 545.9, [Na^+] = 468.5, [Mg^{2+}] = 53.08, [SO_4^{2-}] = 28.23, [Ca^{2+}] = 10.28, [K^+] = 10.21 and [HCO_3^-] = 2.3. The temperature was set as 25°C.

 doi:10.20944/preprints202306.0368.v1

2.5. Trace Element Assessments

2.5.1. Sampling and Chemical Analysis of Digestive Gland

32 oysters for each condition were dissected to sample gills (for metabolomic see § 2.1.6), and digestive gland. According to previous studies, digestive gland is the soft tissue in which the highest trace metal contamination occurs, for many mollusks including oysters, [15–17]. This is of particular interest when the detection targets less concentrated metals like In^{3+}. Each digestive gland was carefully dissected out as quickly as possible on ice. Subsequently, the glands were weighed to obtain the fresh weight, then dried (48h at 50°) before acid digestion. Around 250mg of samples were weighed and were digested using a 6:2 (v/v) 67–70% HNO3/34–37% HCl mixture (Fisher, trace metal quality). Sample acidic digestion was carried out overnight at room temperature and then in a Milestone Ehos Up microwave oven (30 min with constantly increasing temperature up to 120 °C, then hold 15 min at this temperature). Each sample was made up to 50 mL with ultrapure quality water. Analyses of Al, Zn and In were performed [7] with a Agilent 5800VDV ICP-AES and a Thermofisher Scientific XSeries 2 ICP-MS.

A standard certified value sample, DOLT5 (Dogfish liver) was used to validate the analytical method. Average recovery percentages are given relative to the certified values for Al (97% ± 0.07 µg/g Dry Weight) and Zn (101% ± 0.02 µg/g Dry Weight). For indium, no certified organic sample was available.

2.5.2. Chemical Analysis of Passive Samplers

Four passive samplers with the reference LSNM-NP open-pore Loaded DGT device for metals (A) in solution (DGT®Research) were successively collected per tank (every four days) to determine total concentrations of Al, Zn and In (see § 2.5.2).

The passive samplers were opened in a clean-air environment and the binding phase (Chelex 100 resin gel) was peeled off and eluted with ultrapure nitric acid (1 M). Analyses of Al, Zn and In were performed with an Agilent 5800VDV ICP-AES and a Thermofisher Scientific XSeries 2 ICP-MS [7].

2.5.4. Statistical Analysis

Potentially significant differences ($p<0.05$) in trace elements in both digestive gland and passive samplers were tested between the three conditions (control, Zn-anode and Al-Zn-In- anode) using the non-parametric Kruskal-Wallis' test and PAST software.

2.6. Metabolomic Sample Analysis

2.6.1. Tissue Sample Preparation

Each sample was prepared from the gills of two to three oysters, which were dissected, dried on absorbent paper and snap-frozen in liquid nitrogen as described in the publication by Ory and collaborators [18]. Thus, a total of 13 control, 13 Zn-exposed and 14 Al-exposed samples were obtained. Gills in bivalves form the main interface between the organism and the surrounding water and have become therefore a key organ for food absorption. Given the high-water filtration rates of bivalves, gills constitute also a significant pathway of incorporation of pollutants and among them metals via seawater [19]. It has been shown that gills would have high defense ability against contaminants, with a notable presence of antioxidant enzymes and metallothioneins in particular [20]. Consequently, gills play a central role in scenarios of acute exposure to metals, by integrating both absorption and metabolism. The samples were then crushed on ice and adjusted to 1 g. To extract a maximum of compound, each sample was subjected to a triple acetone/acetone/methanol extraction as previously described [21,22]. The three solvent supernatants obtained were then pooled. To remove residual impurities, they were centrifuged at 3000 x g for 5 min. This total supernatant was recovered and dried under a stream of nitrogen as previously described [21,22]. The dry extract was finally resuspended in 2 mL of 20/80 methanol/water, then diluted ten times in water, centrifuged 5

 doi:10.20944/preprints202306.0368.v1

minutes at 13 000 rpm and filtered at 0.2 µm (using low protein binding filter) before MS analyses. The methanol and acetone used were of HPLC grade purity (CARLO ERBA Reagents, Val-de-Reuil, France).

2.6.2. UHPLC/QToF MS Analysis of Samples

An ultra-high performance liquid chromatography ("Acquity UPLC H-class", Waters, Milford, CT, USA) coupled to high resolution mass spectrometry equipped with an electrospray ionization source was used to analyze the samples ("XEVO-G2-S Q-TOF", Waters, Manchester, UK). 5 µL of the samples were injected in a column "Acquity UPLC HSST3" (Waters) (2.1 x 150 mm, 1.8 µm), and the products were eluted at a flow rate of 300 µL/min using a gradient composed of solvents A (water/formic acid 100/0.001 (v:v)) and B (acetonitrile/formic acid 100/0.001 (v:v)), according to the following procedure: 0–3 min, 100% A; 3–8 min 0–50% B; 8–13 min 50% B; 13–20 min 50–95% B; 20–30 min, 95% B, 30–31 min 95–0% B, 31–37 min 100% B. The analyses were performed in positive and negative ionization modes with MS function in a centroid mode. For the two ionization modes, the MS parameters applied in the ESI source were: source temperature 120 °C, desolvation temperature 500 °C, gas flowrate of the cone 50 L/h, desolvation gas flowrate 800 L/h. Capillary voltage was 3 kV (+) and 2.5 kV (-) and sampling cone 35 V. The instrument was adjusted for the acquisition on a 50–1200 m/z interval, with a scan time of 0.1 s. To identify ions of interest, targeted MS/MS were achieved using a collision energy ramp varying from 10 to 60 eV depending on molecules The Leucine Enkephalin (M = 555.62 Da, 1 ng/µL) was used as a lock-mass and the mass spectrometer was calibrated using 0.5 mM sodium formate solution. The samples were analyzed randomly to avoid the effect of possible analytical drift. Analytical repeatability was guaranteed by quality control samples (QC) that were injected every five measurements. The QCs were obtained from the pooling of all samples. Blanks prepared with the last extraction solvent were injected at the beginning and end of the sample sequence to subtract components from the extraction solvent.

2.7. Statistical Analysis

The data were processed as ion peak intensity using the Workflow4Metabolomics(W4M) platform (http://workflow4metabolomics.org, accessed on 10 December 2021) according to the method described by Ory and collaborators [22]. Analytical drift was corrected on the pools, using a Loess regression model [23]. Repeatability was assessed through the coefficient of variation (CV) of the QCs. Metabolites with a CV > 0.3 were removed from the analyses. Principal component analysis (PCA) was used to detect natural clustering between samples. Partial least squares-discriminant analysis (PLS-DA) was performed on the log-transformed and Pareto normalized data. The selection of metabolites was based on the importance of their contribution as a predictor variable in the PLS-DA model, as evaluated by their Variable In Projection (VIP). A data with variable in projection (VIP) > 1 can be considered as a metabolite having a significant contribution to the PLS-DA model. The evaluation parameters of the model (R2Y, Q2) were obtained through 7-fold cross-validation, and the permutation test (n = 100) was used to measure the effectiveness of the model. This last test consists of keeping the data set constant, while randomly permuting the order of the pre-defined variables a set number of times. Student's t-test were then applied to evaluate the significance of differential metabolites, with a rejection threshold of 5%.

2.8. Metabolite Identification

After targeted MS/MS of discriminant metabolites, ion spectra corresponding to their fragmentation profiles were uploaded into the identification software Sirius4 [24]. First, the molecular formula determination was achieved by Sirius with C, H, O, N, P, S as allowed elements and MS^2 mass accuracy was fixed at 20 ppm. Then, the tool 'Predict FPs' was used to predict the molecular fingerprints of compounds and 'Search DBs' was used to search compounds in all proposed structure databases (CSI:FingerID). Finally, 'CANOPUS' was used to predict compounds' class. Molecular

Preprints (www.preprints.org) | NOT PEER-REVIEWED | Posted: 6 June 2023 doi:10.20944/preprints202306.0368.v1

formulas were accepted if Sirius scores were > 95% and a minimum similarity of 60% was used to restrict the proposed compound structures.

Analytical standards were used and analyzed according to the same method as explained above to check the identification of proline, phenylalanine and betaine (Sigma-Aldrich, Darmstadt, Germany). Comparison of these standards (retention times, m/z and fragments) with the QC validates the identification of these ions (Figure 3).

Finally, we used the classification of Shymanski *et al.*, to support the identification of the metabolites [25]. This method assigns a score to each metabolite based on the degree of confidence in its identification [25]:

- Score 1, identification using a standard (same retention times, m/z and fragments).
- Score 2a, annotation using fragmentation data from all databases proposed by Sirius with an unambiguous spectrum-structure match.
- Score 2b, the fragments obtained match completely with the proposed structure, which excludes other possibilities, but the data are not completely available in the databases.
- Score 3, proposed annotation of one or more isomeric molecules without the possibility of distinguishing between them because few or no fragments were obtained, or the fragments were common to the different positional isomers.

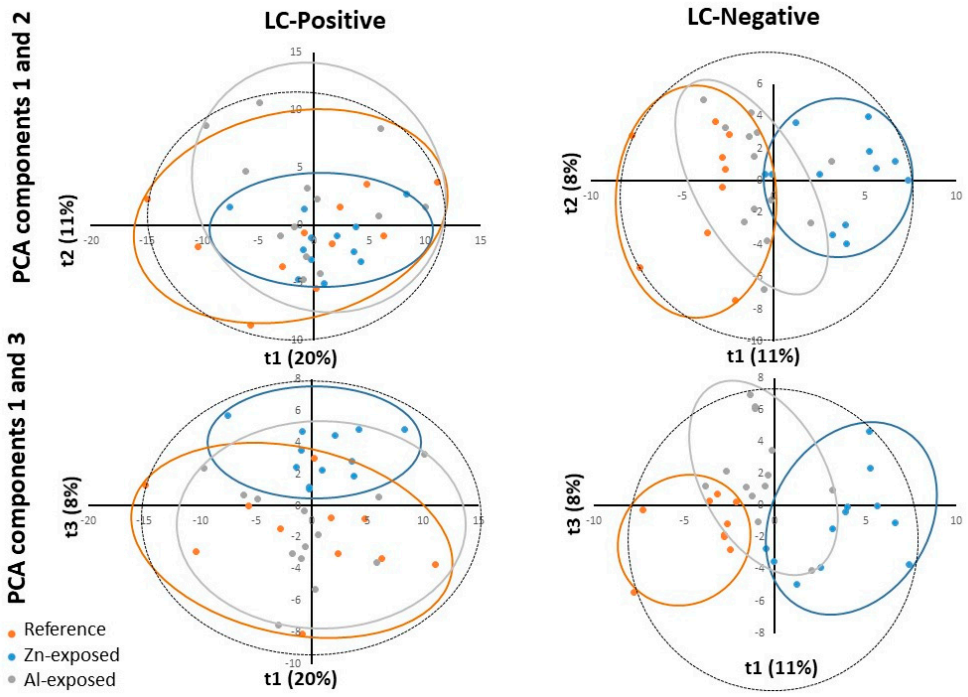

Figure 2. The PCA scores of the oyster samples in each group with the ESI positive (LC-Positive) and negative (LC-Negative) ion modes. t1 represents principal component 1, t2 represents principal component 2 and t3 represents principal component 2. The dotted ellipse represented the confidence limit (95%) of Hotelling's T2 statistic. The reference samples ("Reference"), the Zn-anode exposed ("Zn-exposed") and the Al-Zn-In anode exposed ("Al-exposed") samples are visually grouped in orange, blue and grey ellipses, respectively.

Preprints (www.preprints.org) | NOT PEER-REVIEWED | Posted: 6 June 2023 doi:10.20944/preprints202306.0368.v1

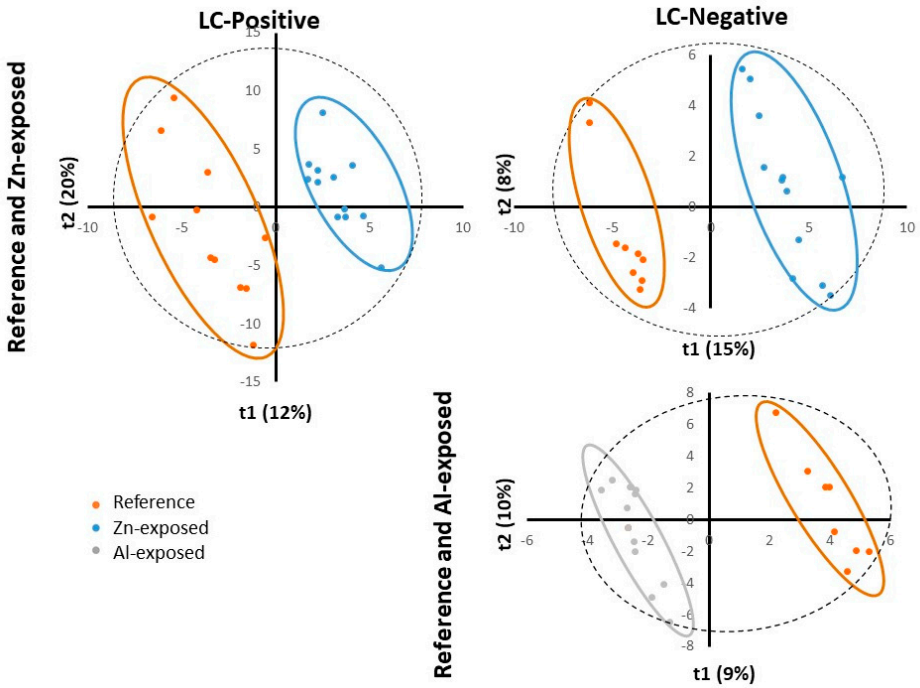

Figure 3. PLS-DA scores plotted for Reference and Zn-exposed samples for ESI positive (LC-Positive) and negative (LC-Negative) ion modes (top) and for Reference and Al-exposed samples for ESI negative (LC-Negative) ion mode (bottom). t1 represents principal component 1, t2 represents principal component 2 and t3 represents principal component 2. The dotted ellipse represented the confidence limit (95%) of Hotelling's T2 statistic. The reference samples ("Reference"), the Zn-anode exposed ("Zn-exposed") and the Al-Zn-In anode exposed ("Al-exposed") samples are visually grouped in orange, blue and grey ellipses, respectively.

3. Results

3.1. Chemical Modelling of Species, Corresponding to the Degradation Products of the Al-Zn-In- and Zn-Anodes

The exact nature and solubility of the corrosion products formed in seawater from Al-Zn-In galvanic anodes is not clearly established yet. As a first approach, a chemical modelling was carried out considering $Al(OH)_3$ and $Zn(OH)_2$ as the solid phases in equilibrium with the solution. For $Al(OH)_3$, two cases were considered that may correspond to two extreme situations. First, amorphous $Al(OH)_3$ was chosen as the less stable, i.e., the more soluble, solid phase likely to form. Upon ageing, it would tend to a better crystallinity and gibbsite, the most stable $Al(OH)_3$ polymorph, was chosen as the less soluble compound likely to form. For zinc hydroxide, only the most stable polymorph, i.e., ε-$Zn(OH)_2$, was considered. The results are gathered in Table 1.

Two equilibrium pH values were considered in the pH range of seawater, namely 8.0 and 8.2. The results show opposite trends for the solubility of $Zn(OH)_2$ and $Al(OH)_3$. As revealed by the decrease of Al dissolved species concentration, the solubility of $Al(OH)_3$ decreases when pH decreases from 8.2 to 8.0. Conversely, the Zn dissolved species concentration increases when the pH decreases from 8.2 to 8.0. Due to the galvanic coupling with the protected steel structure, the oxidation of the anode is faster than the reduction of dissolved O_2 so that the production rate of metal cations (Al^{3+} and/or Zn^{2+}) is higher than the production rate of OH^- ions. In other words, the $[Al^{3+}]/[OH^-]$ ratio is higher than 3 and the $[Zn^{2+}]/[OH^-]$ ratio is higher than 2. A decrease of pH is then expected at the vicinity of the anode, as the cations, in particular Al^{3+}, are acid species. Consequently, the solubility of $Zn(OH)_2$ should be increased by this effect while that of $Al(OH)_3$ should be decreased. More detailed chemical modelling studies can be found [26], which show that the lowest solubility

Preprints (www.preprints.org) | NOT PEER-REVIEWED | Posted: 6 June 2023 doi:10.20944/preprints202306.0368.v1

for $Al(OH)_3$ is reached at pH = 7 and increases importantly for pH values below 5.5 or higher than 8.5 [26].

Table 1. Chemical modelling: dissolved species concentrations computed for two pH values, corresponding to the equilibrium conditions with the considered solid phase (concentrations given in µg/kg), main dissolved species and relative abundance (R.A.) and a list (not exhaustive) of other dissolved species with corresponding R.A.

Equilibrium solid phase	**Amorphous $Al(OH)_3$**	**Amorphous $Al(OH)_3$**	**Gibbsite**	**Gibbsite**	**ε-$Zn(OH)_2$**	**ε-$Zn(OH)_2$**
pH	8.0	8.2	8.0	8.2	8.0	8.2
Dissolved species conc.	5153	8410	17	26	21582	9614
Main dissolved species	$Al(OH)_4^-$	$Al(OH)_4^-$	$Al(OH)_4^-$	$Al(OH)_4^-$	Zn^{2+}	Zn^{2+}
R.A.	99.4 %	99.6 %	99.45 %	99.65 %	34.3 %	30.7 %
Other dissolved species and R.A.	$Al(OH)_3^0$ (0.5 %) $Al(OH)_2^+$ (0.04 %)	$Al(OH)_3^0$ (0.33 %) $Al(OH)_2^+$ (0.015 %)	$Al(OH)_3^0$ (0.5 %) $Al(OH)_2^+$ (0.035 %)	$Al(OH)_3^0$ (0.33 %) $Al(OH)_2^+$ (0.015 %)	$ZnCl^+$ (16.9 %) $ZnOHCl^0$ (14.0 %) $Zn(SO_4)_2^{2-}$ (8.1 %)	$ZnOHCl^0$ (19.9 %) $ZnCl^+$ (15.1 %) $Zn(SO_4)_2^{2-}$ (7.3 %)

When dealing with $Al(OH)_3$, it is also clearly observed that the ageing of the initial precipitate, that is amorphous $Al(OH)_3$, and the subsequent increased crystallinity, would drastically change the solubility of the solid phase. Upon ageing, the dissolved Al concentration in equilibrium with the solid phase would tend to decrease from about 5000-8000 µg of Al per kg of water to 17-26 µg/kg of Al per kg of water for the well crystallized gibbsite polymorph. In contrast, no such important evolution of crystallinity was reported for Zn hydroxide so that the dissolved species concentration in equilibrium with the solid phase keeps the same order of magnitude, i.e., about 10000-20000 µg of Zn per kg of water.

Finally, the main dissolved species are also different when comparing Al and Zn. At both considered pH values, the main Al dissolved species is the $Al(OH)_4^-$ anion, which represents more than 99% of the dissolved Al species. The remaining 1% mainly corresponds to the neutral complex $Al(OH)_3^0$ and to the cation $Al(OH)_2^+$. The modelling also showed that the concentration of the Al^{3+} cation was negligible, i.e., about 10^{-12} mol/kg in any case. For Zn, the main dissolved species is the cation Zn^{2+} (30-35% of the dissolved species). Other important dissolved species are the cation $ZnCl^+$, the neutral complex ZnOHCl° and the anion $Zn(SO_4)_2^{2-}$.

To conclude this section, note that these results only give general informative trends as the concentration and nature of dissolved Al and Zn species in equilibrium with the solid phase do not depend only on the considered solid phase (as illustrated here for Al) or on pH, but also on temperature, seawater composition and in particular on the presence and amount of organic matter or other Al-ligands [26] and Zn-ligands.

3.2. Levels of Trace Elements

Seawater was continuously renewed from the experimental marsh. The use of passive samplers assessed that the water supplied to the tanks contains no detectable quantities of aluminum, indium or zinc in dissolved form. The analysis of the metal species in their soluble form confirms that in our

Preprints (www.preprints.org) | NOT PEER-REVIEWED | Posted: 6 June 2023 doi:10.20944/preprints202306.0368.v1

experimental conditions, aluminum or zinc is the main ion released by Al-Zn-In-anode or Zn-anode respectively (Table 2).

Table 2. Al, In and Zn concentrations (µg/sampler) measured in the dissolved fraction using passive samplers. Each sampler is immersed for four days out of the 16 days of experimentation in tank control or equipped with Al-Zn-In-anode or Zn-anode. Mean ± standard deviation. d.l = detection limit.

µg/sampler	Control (n=4)	Al-Zn-In-anode (n=4)	Zn-anode (n=4)
Al	< d.l	**148 ± 22**	< d.l
In	< d.l	< d.l	< d.l
Zn	< d.l	< d.l	**360 ± 125**

Under all conditions, the analysis of aluminum concentration in digestive gland does not show any significant difference (Table 3) after 16 days of exposure. In the same way, digestive glands obtained from oysters exposed to the product released by Al-Zn-In-anode or Zn-anode do not show significant accumulation of zinc compared to control ones while indium is below the detection values.

Table 3. Concentrations (± SD) of aluminum, indium or zinc (µg/g dry weight) measured in digestive glands of *M. gigas* placed in control condition or exposed for 16 days to Al-Zn-In-anode or Zn-anode. Mean ± standard deviation. d.l = detection limit.

µg/g dry weight (digestive gland)	Control (n=32)	Al-Zn-In-anode (n=32)	Zn-anode (n=32)
Al	39.9 ± 12.1	29 ± 12.9	28 ± 11.5
In	< d.l	< d.l	< d.l
Zn	1590 ± 459	1348 ± 164	1718 ± 271

3.3. LC/MS Data Processing and Analyses

XCMS preprocess from Workflow4Metabolomics platform (W4M) allowed the detection of 1,309 and 958 and m/z features for positive and negative ionization modes, respectively. Then data process implied blank removal and batch correction to eliminate instrument signal drift and offset differences between batches. Sample intensities were adjusted using a Loess regression model fitting with the pool values. We evaluated the analytical repeatability of metabolite intensity dataset by calculating coefficients of variation (CV) detected in the Quality Control samples (QC = pool of all samples) and metabolites with CV > 0.3 were removed from the datasets. These different data process steps led to keep 1147 and 871 ions in positive and negative ionization modes, respectively. Multivariate analyses were then performed on these latter datasets.

First, Principal Component Analyses (PCA) showed the sample distribution based on the qualitative and quantitative metabolites composition, highlighting the natural structure of samples (Figure 1).

For LC/MS positive mode, the reference group, Zn-anode and Al-Zn-In anode exposed groups did not show obvious trends of separation, when considering the two first principal components (PC) of the PCA score plot, PC1 and PC2 explaining 20% and 11% of the total variability respectively. However, when considering PC3, which explained 8% of the total variability, PCA score plot described a clustering trend for the reference and the Zn-anode exposed group, but no clustering trend appeared between the Al-Zn-In group and the other groups.

For LC/MS negative mode, variable metabolite presence and intensities, as shown through PC1 and PC2 plot (11% and 8% of the total variability respectively) induced a clear clustering of reference

Preprints (www.preprints.org) | NOT PEER-REVIEWED | Posted: 6 June 2023 doi:10.20944/preprints202306.0368.v1

and Zn-anode exposed groups, while Al-Zn-In anode exposed group lay between these two groups with common areas with both groups. When considering PC3 (8% of the total variability), a clustering trend for the Al-Zn-In anode exposed group from the two other groups appeared.

In summary, on the score plot, the PCA showed a natural clustering between reference and Zn-anode exposed samples, for both positive and negative modes, justifying PLS-DA model reliability for both modes. For reference and Al-Zn-In anode groups the separation appeared only for negative mode and PLS-DA was only carried out in this case.

PLS-DA is a supervised method, which builds a model that forces the distinction between two firstly defined groups. PLS-DA analyses were first performed to identify metabolites whose abundance was related to exposure to Zn-anode, in the two datasets negative and positive modes. The relevance and performance of the supervised built model was proven with PLS-DA parameters of data consistency (R2) and prediction performance (Q2). R2 (cumulative) reached more than 0.99 for both ionization modes and Q2 (cumulative) reached 0.792 and 0.811 for positive and negative modes, respectively. Permutation test (n = 100) and cross-validation test provided p-values < 0.05 confirming the consistency of the data and the reliability of the predicted models. Thus, a separation between the reference and Zn-anode exposed groups was significantly demonstrated.

PLS-DA also provides results of variables responsible for forced clustering. Among variables structuring the sample distribution of PLS-DA model, Variable Importance in Projection (VIP) >1 defined the ones with the significant contribution to the variance between the control and exposed groups. We kept metabolites with VIP >1 and obtained 255 and 225 metabolites for positive and negative modes respectively. Among them 119 and 124 ions for positive and negative modes respectively showed a significant difference between the reference samples and the samples exposed to Zn-anode (t-test or Mann-Whitney test, p-value <0.05). Among them, 16 metabolites were identified by using one of the identification methods described in the "Materials and methods" section.

PLS-DA analyses were then performed to identify metabolites whose abundance was related to exposure to Al-Zn-In anode, in the dataset of negative mode. The relevance and performance of the supervised built model was proven with PLS-DA parameters of data consistency (R2) and prediction performance (Q2). R2 (cumulative) reached more than 0.99 and Q2 (cumulative) reached 0.71. Permutation test (n = 100) and cross-validation test provided p-values < 0.02 confirming the consistency of the data and the reliability of the predicted models. Thus, a separation between the metabolite composition of the reference and Al-Zn-In anode exposed groups was significantly demonstrated. We kept metabolites with VIP >1 and obtained 262 ions. To improve the prediction performance of the model and to select the variables presenting the most important contribution in the classification model, a supplementary PLS-DA model was built with only variables with VIP > 1, reaching Q2=0.903. This allowed the selection of 82 ions.

Among them 63 showed a significant difference between the reference samples and the samples exposed to Al-Zn-In anode (t-test or Mann-Whitney test, p-value <0.05) but only 2 were strongly identified.

3.4. Metabolites Modulation

3.4.1. Modulations Observed for Zn-Anode Exposed Oysters

The use of the different online databases mentioned above or comparison with standards allowed the confirmed identification of 16 metabolites. Indeed, their scores were less or equal to 2a in Shimanski scale (Table 4), except for the eicosanoids, a family of compounds for which a more precise annotation was not possible. Among the 16 identified metabolites, three have a confirmed structure (score 1): proline, betaine and phenylalanine. Among them, four were annotated in negative ionization mode, eight in positive ionization and four were annotated in both ionization modes (Table 4). They belong to four different biochemical classes: seven are amino acids or derivatives, three are nucleotides or nucleosides, two are carnitine or derivatives and four are various. These 16 metabolites are significantly modulated between reference and Zn-anode exposed oysters (Figure 4).

Preprints (www.preprints.org) | NOT PEER-REVIEWED | Posted: 6 June 2023 doi:10.20944/preprints202306.0368.v1

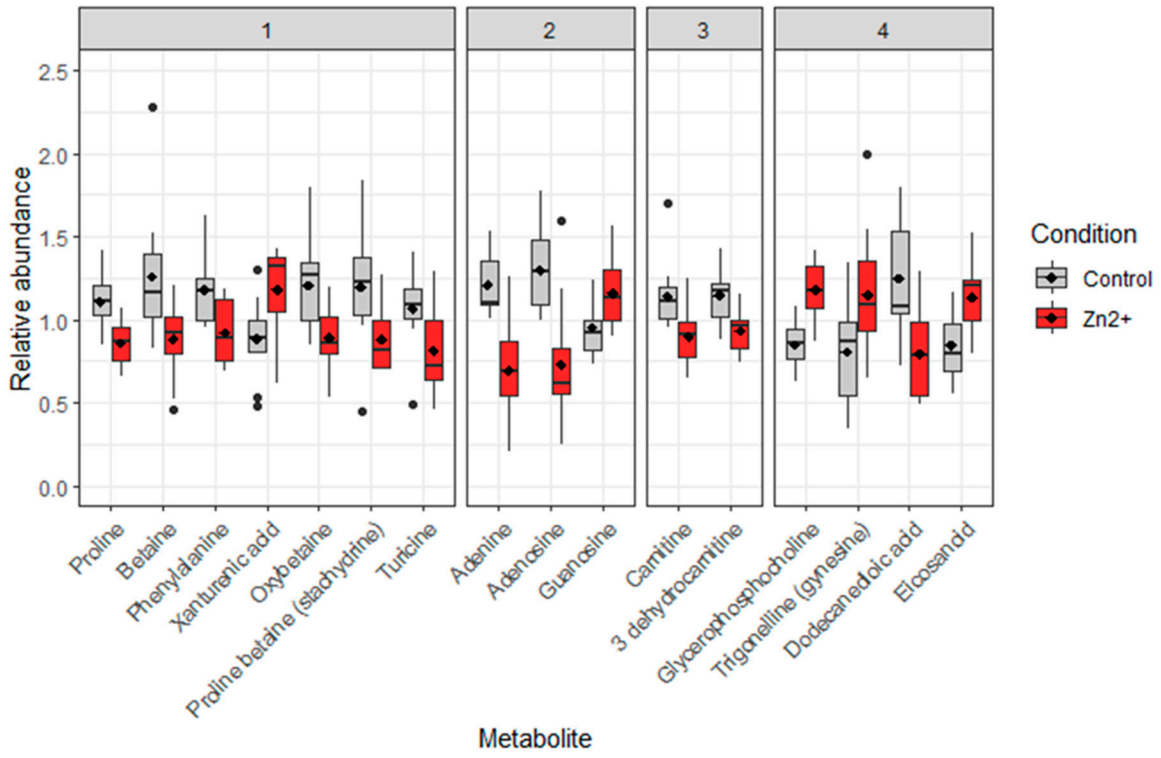

Figure 4. Box plots of the relative abundance of significant compounds (16 identified by the PLS-DA model (Figure 3)) in *M. gigas* gills. Grey plots represent the reference samples, red plots represent data obtained on oysters exposed to the dissolution of Zn-anode (the mean value is given by the dark diamond-shaped symbol). Metabolite has been classified by family: Group 1: Amino acids and derivatives; Group 2: Nucleotides and nucleosides; Group 3: Carnitine acids and derivatives; Group 4: Others.

The complete list of annotated metabolites is presented in Table 4. Most of them were down-regulated (percentage change of relative abundance; mean ± SD): six amino acids or derivatives (-25,7 ± 2.7%); adenine and adenosine (-34,1 ± 10.5%) for nucleotides and nucleosides group, two metabolites for carnitine and derivatives group (-19 ± 1.9%) and only dodecanedioic acid (-58.6%) for the last group. Some metabolites are also up regulated like xanthurenic acid (in positive mode) and xanthurinate (in negative mode) with a +64.5 ± 44.4% modulation, guanosine (nucleotide and nucleoside group) +21.5% modulation, and two metabolites and a family of compounds (glycerophosphocholine, trigonelline and metabolite from eicosanoids family, 38.7 ± 4.1%) belonging to the last group ("others")

3.4.2. Modulations Observed for Al-Zn-In Anode Exposed Oysters

The use of the different online databases mentioned above or comparison with standards allowed the confirmed identification of two metabolites (Table 5) among the 63 ions showing a significant difference between the reference samples and the samples exposed to Al-Zn-In anode (t-test or Mann-Whitney test, p-value <0.05. L-phenylalanine was down-modulated in Al-Zn-In anode exposed samples compared to reference (–23,3% of relative abundance, p = 0.002) whereas the metabolite from eicosanoid family is up-regulated (+34,6%, of relative abundance p = 0.002) (Figure 5). Among the 61 remaining ions, 31 were also present in the list of ions showing a significant difference between the reference samples and the samples exposed to Zn-anode but could not be identified. 13 were also present in the list of ions showing a difference between the reference samples and the samples exposed to Zn-anode, but not significant and only 18 ions were specific to Al-Zn-In anode.

Table 4. Significant metabolites modulation detected in gills of *M. gigas* after chronic exposure for 16 days of the product of Zn-anodes dissolution. Metabolites are classified by family. The power of modulation is given by the multiplication factor (Zinc effect). The up arrows represent up-modulations, and the down-arrows are for down-modulations. The score represents the Shymanski classification.

Group	Metabolite	Mode	Retention time (min)	Formula	Adduct	Monoisotopic Mass (Da)	Observed Mass (*m/z*)	Theoretical Mass (*m/z*)	Mass Error (ppm)	Score	Zn^{2+} effect	
Amino acids and derivatives	Proline	Pos/Neg	1,36/1,35	$C_5H_9NO_2$	$[M^+H]^+/[M^-H]^-$	115,0633	116,0712/114,0553	116,0706/114,0561	5,4/7,0	1	0,8/0,7	↘
	Betaine	Pos	1,26	$C_5H_{11}NO_2$	$[M^+K]^+$	117,0795	156,0424	156,0432	5,6	1	0,7	↘
	Phenylalanine	Neg	6,52	$C_9H_{11}NO_2$	$[M^-H]^-$	165,0795	164,0709	164,0722	8,1	1	0,8	↘
	Xanthurenic acid/Xanthurinate	Pos/Neg	7,42/7,34	$C_{10}H_7NO_4$	$[M^+H]^+$/Isotope of $[M^-CO_2^-H]^-$ at 160.0396	205,0375	206,0454/160,0396	206,0448/160,0404	3,2/5,2	2a	1,3/2,0	↗
	Oxybetaine	Pos	1,29	$C_6H_{14}NO^{3+}$	$[M]^+$	148,0974	148,0971	148,0974	2,1	2a	0,7	↘
	Proline betaine (stachydrine)	Pos	1,21	$C_7H_{14}NO^{2+}$	$[M]^+$	144,1019	144,1025	144,1019	3,9	2a	0,7	↘
	Turicine	Pos	8,67	$C_7H_{13}NO_3$	$[M^+H]^+$	159,0895	160,0968	160,0968	0,0	2a	0,8	↘
Nucleotides and nucleosides	Adenine	Pos/Neg	6,79/6,74	$C_5H_5N_5$	$[M^+H]^+/[M^-H]^-$	135,0545	136,0621/134,0463	136,0618/134,0472	2,5/6,5	2a	0,7/0,6	↘
	Adenosine	Pos/Neg	6,79/6,74	$C_{10}H_{13}N_5O_4$	$[M^+H]^+/[M^-H]^-$	267,0968	268,1046/266,0886	268,1040/266,0895	2,3/3,2	2a	0,8/0,6	↘
	Guanosine	Neg	6,52	$C_{10}H_{13}N_5O_5$	$[M^-H]^-$	283,0917	282,0839	282,0844	1,7	2a	1,2	↗
Carnitine and	Carnitine	Pos	1,18	$C_7H_{16}NO^{3+}$	$[M]^+$	162,1125	162,1130	162,1125	3,3	2a	0,8	↘
	3-dehydrocarnitine	Pos	1,33	$C_7H_{16}NO^{2+}$	$[M]^+$	146,1176	146,1179	146,1176	2,3	2a	0,8	↘
Others	Glycerophosphocholine	Pos	1,21	$C_8H_{20}NO_6P$	$[M^+H]^+$	257,1028	258,1105	258,1101	1,7	2a	1,4	↗

doi:10.20944/preprints202306.0368.v1

Trigonelline (gynesine)	Pos	1,54	$C_7H_7NO_2$	Isotope P^{+2} of $[M^+H]^+$	137,0477	138,0558	138,0550	6,1	2a	1,4	↗
Dodecanedioic acid	Neg	11,23	$C_{12}H_{22}O_4$	$[M-2H^+Na]^-$	230,1518	251,1273	251,1265	3,2	2a	0,4	↘
Eicosanoid	Neg	10,85	$C_{20}H_{32}O_5$	$[M-H]^-$	352,2250	351,2172	351,2177	1,5	3	1,3	↗

Table 5. Metabolites modulation detected in gills of *M. gigas* after chronic exposure for 16 days of the product of Al-Zn-In-anode dissolution. Metabolites are classified by family. The power of modulation is given by the multiplication factor (Al-Zn-In effect). The up arrows represent up-modulations and the down-arrow are for down-modulations. The score represents the Shymanski classification.

Group	Metabolite	Mode	Retention time (min)	Formula	Adduct	Monoisotopic Mass (Da)	Observed Mass (*m/z*)	Theoretical Mass (*m/z*)	Mass Error (ppm)	Score	Al-Zn-In effect	
Amino acids and derivatives	Phenylalanine	Neg	6,52	$C_9H_{11}NO_2$	$[M-H]^-$	165,0795	164,0709	164,0722	0,8	1	0,8	↘
Others	Eicosanoid	Neg	10,85	$C_{20}H_{32}O_5$	Isotope at 351.2166/$[M-H]^-$	352,2250	351,2166	351,2177	3,1	3	1,3	↗

doi:10.20944/preprints202306.0368.v1

Preprints (www.preprints.org) | NOT PEER-REVIEWED | Posted: 6 June 2023 doi:10.20944/preprints202306.0368.v1

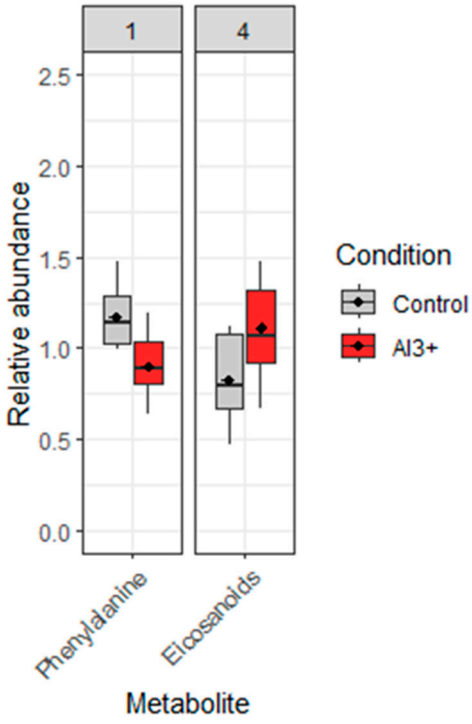

Figure 5. Box plots of the relative abundance of significant compounds (2 identified by the PLS-DA model (Figure 3)) in *M. gigas* gills. Grey plots represent the reference samples, red plots represent data obtained on oysters exposed to the dissolution of Al-Zn-In-anode (the mean value is given by the dark diamond-shaped symbol). Metabolite has been classified by family: Group 1: Amino acids and derivatives; and Group 4: Others.

4. Discussion

To our knowledge, the present study is the first study using a metabolomic approach to evaluate the effects of metals released by galvanic anode on oysters and combining this metabolomic approach with a chemical modelling study of degradation products from these anodes. The comparative effects of Zn- and Al-Zn-In- anodes were carried out under experimental conditions without sediment and with an important water renewal.

4.1. Chemical Modelling and Its Implications

The computed dissolved species concentrations given in Table 1 correspond to the equilibrium conditions between the considered solid phase and the solution. Such concentrations would be reached in the immediate vicinity of the anode, inside the porous layer of corrosion products surrounding the metal and (maybe) a few centimeters away from the anode surface. They correspond to a maximum value and the dissolved species concentration is expected to decrease with the distance from the anode down to the low value typical of bulk seawater. The concentration profile should mainly be linked to the hydrodynamic conditions.

Al and Zn could also be carried away from the anode as fragments of the solid phase. Such solid particles may accumulate locally in the environment, for instance in confined areas where stagnant conditions could be met. In this situation, the solid particles falling from the anode would accumulate in the seabed below. The subsequent dissolution of these particles would then lead to a local enrichment in Al and/or Zn dissolved species. In the experimental conditions considered here (Figure 1), the oysters were scattered around the water outlet of the tank. The solid particles detaching from the corrosion product layer covering the anode were then carried away by the seawater flow towards the oysters.

Preprints (www.preprints.org) | NOT PEER-REVIEWED | Posted: 6 June 2023 doi:10.20944/preprints202306.0368.v1

In the case of Al-Zn-In anodes, both Al and Zn ions are released in solution. The Al and Zn dissolved species concentrations are controlled by the solubility of the respective solid phases (Table 1). Consequently, due to the higher solubility of $Zn(OH)_2$ with respect to $Al(OH)_3$, the dissolved Zn species concentration at the vicinity of an anode could be higher than the Al dissolved species concentration, even though the anode contains only 3-5 wt.% Zn and is mainly composed of Al. The main Al dissolved species coming from galvanic anode dissolution is the $Al(OH)_4^-$ anion, which represents more than 99% of the dissolved Al species at the pH of seawater. For Zn, the main dissolved species is the cation Zn^{2+} (30-35% of the dissolved species), other important dissolved species being the complex ions $ZnCl^+$, $ZnOHCl°$ and $Zn(SO_4)_2^{2-}$. It is not possible to accurately assess the amounts of soluble Al and Zn species to which oysters are exposed, as solid Al and Zn particles may accumulate near the oysters and subsequently dissolve. However, as mentioned earlier, there could be a higher level of exposure to Zn^{2+} ions than to $Al(OH)_4^-$ ions, when using Al-Zn-In anodes.

In the case of Zn-anode, it can be stated that the quantities of Zn^{2+} ions to which oysters are actually exposed to are higher than in the case of Al-Zn-In anodes, higher even than the sum of the individual ions coming from the latter anode. This would result from the higher amount of $Zn(OH)_2$ particles produced and released in the environment, and from the relatively high solubility of $Zn(OH)_2$.

However, the quantities of Zn^{2+} and Al^{3+} ions to which bivalves are exposed when using galvanic anodes are much lower than the corresponding quantities afforded from sulphate salts. This is consistent with a study performed in 2010, showing that the dissolution of Al and Zn from a galvanic anode was less toxic for the urchin *Paracentrotus lividus* than sulphate salts [5].

4.2. Bioaccumulation

The use of passive samplers confirms the higher quantity of dissolved form of aluminum or zinc in tanks equipped respectively with Al-Zn-In anodes and Zn anode. For indium, it could not be detected. However, neither oysters exposed to the corrosion of Zn-anode nor those exposed to the corrosion to Al-Zn-In- anode accumulate Zn or Al in their digestive gland. Caplat et al. (2012) showed that the digestive gland of *M. gigas* has a great capacity to accumulate zinc released by a sacrificial anode made of Zinc [27]. However, according to their experimental design, the concentration of zinc to which their oysters were exposed was much higher than in our conditions. Under their conditions, the digestive glands of oysters exposed to the product of sacrificial anode exhibited an increase in zinc concentration after 21 days of exposure, when the external nominal zinc concentration was about 0.3 ± 0.04 mg/L and after 96h when the external nominal zinc concentration was about 10.2 ± 1.2 mg/L [27].

Concerning the bioaccumulation of degradation products from anodes mainly composed of Al, very few studies were performed on marine bivalves.

In a first study, the concentration of aluminum was measured in digestive gland of mussels *Mytillus edulis* exposed to sacrificial anode composed mainly of aluminum (93.2% min aluminum, 2.73 kg/dm density) [28]. Seawater was continuously renewed, and the nominal aluminum concentration fluctuate between 270 and 810 µg/L in their experimental conditions. At the maximum, obtained on the 13th day of contamination, they found that digestive gland of exposed mussels concentrated about four times more Al than non-exposed ones and six times more Al than the total soft tissues. Our experimental conditions exposed our oysters to a much lower level of aluminum (80 µg/L of Al^{3+} released from the anode). After 16 days of experimentation, the digestive gland of oysters exposed to Al-Zn-In anode did not show any bioaccumulation of Al^{3+}, nor Zn^{2+} or other metal cations like In^{3+}.

In a second study, Levallois et al. worked on the bioaccumulation of Zn and Al in oysters after an 84-day exposure to Al-based anodes like our Al-Zn-In anodes [8]. They found that bivalves bioaccumulated more zinc than aluminum (in total tissues), even if nominal aluminum concentrations during exposures were higher. Moreover, exposure time did not influence the bioaccumulation of aluminum in contrast to zinc. Al presented close and lowest bioconcentration factors (BCF) values, whereas Zn BCF values increased in relation to the decrease of exposure

 doi:10.20944/preprints202306.0368.v1

concentrations [8]. BCF measures the ability of an organism to bioconcentrate an element in its tissue considering the concentration of that element in the water. If we want to compare our Al and Zn bioaccumulation results in presence of Al-Zn-In anodes with those of these authors, under conditions most like ours, we must consider their results after 7 and 29 days for nominal Al and Zn exposures of 65 µg/L and 15 µg/L respectively on the one side, and 125 µg/L and 22 µg/L on the other side. Their results showed an approximate doubling of Al levels and a slight increase in Zn concentrations in total flesh compared to controls, whereas we did not observe any differences in the digestive glands after 16 days of exposure to 80 µg/L Al and 4.2 µg/L Zn.

In the present study, the target organ for bioaccumulation is the digestive gland. The digestive gland is a detoxification organ, meaning that metals are taken up, sequestered and transformed into less toxic forms. In our study, no accumulation of any targeted metal was observed after 16 days exposure. The main reasons could be the short duration of exposure, the relatively weak nominal concentrations of product degradation anodes in our conditions and the mainly insoluble character of aluminum. The gills in filter feeders such as oysters have a double role: respiration and feeding organ. They are considerably exposed to metals in soluble form only. This is not the case for grazer species such as limpets (*Patella vulgata*), which are grazers able to ingest also insoluble species. Therefore, it could be interesting to carry out future studies to compare species with different feeding behaviours.

4.3. Ecotoxicological Effects of Zn- and Al-Zn-In- Anodes on Marine Organisms Assessed by Other Methods Than Metabolomics

For now, many studies focused on ecotoxicological effects of Zn- and Al-Zn-In-anodes on marine organisms using classical methods with biomarkers rather than untargeted metabolomic methods. They highlighted interesting and numerous effects on cellular levels (haemocytes), enzyme activities, and transcription levels, but at higher concentrations than those found in the environment, when using sacrificial anodes.

In 2018, Kirchgeorg et al. [30] published a review about emissions from offshore corrosion protection systems and their potential effects on the marine environment. The authors mention that a few studies investigated the fate and the environmental effects of products emitted by the galvanic anodes and that the potential ecotoxicological effects of the different species formed from Al or Zn (hydroxides or complex) still need further investigation to be elucidated. Concerning the data of indium effects in the marine environment, the authors mention that they are rare [29]. The toxicological effects of In on freshwater swamp shrimp (*Macrobrachium nipponense*) was studied and a median lethal concentration for indium (III) between 6.9 and 21.5 mg/L (LC50) was found [30].

Concerning the effect of Zn-anodes, in 2012, Muttin et al. monitored the effects on the Pacific oyster *Magallana gigas* of the degradation products of a sacrificial anode with a minimum of 99.31% zinc, reproducing the same chemical forms of zinc (II) released from anodes as in natural conditions [6]. They performed chronic exposure with 0.5 mg/L Zn for 10 weeks and acute exposure with 10 mg/L Zn for 7 days and analyzed both gills and digestive glands. Chronic exposure led to a decrease of circulating haemocytes and an increase of both phagocytosis capacity and reactive oxygen species (ROS) production. Moreover, phenoloxidase and non-specific esterase activities increased, as was the case for increase for metallothioneins mRNA expression. Acute exposure to high zinc concentration resulted in a high level of mortality, a decrease in the number of circulating haemocytes, an inhibition of immune parameters and a dose- and time-dependent increase of metallothioneins mRNA expression [6]. These results show that several biological functions are affected by exposure to Zn-anodes, as do our metabolomics results (see below). However, they correspond to much higher levels of zinc exposure than ours: twice the nominal concentration for long-term exposure and 34 times higher for short-term exposure.

Concerning the effect of anodes containing Al as major component, their toxicity was studied on the Pacific oyster, *M. Gigas*, in controlled conditions in 2022 [8]. Oysters were exposed for about three months to different Al concentrations obtained with an electrochemical experimental device simulating the dissolution of a galvanic anode. Total Al nominal concentrations were equal to 50, 100

 doi:10.20944/preprints202306.0368.v1

and 300 µg/L got after decantation process (for 24 h) [8]. For the exposure duration, the ROS concentration and the number of circulating hemocytes remained stable. However, after 84 days, a 40% decrease of phagocytic efficiency and stability of lysosomal membranes or change in the number or size of lysosomes were observed at the highest Al concentration, which may indicate a weakened immune system. Moreover, at this highest Al concentration again, the oysters presented significantly lower levels of malondiadehyde in the digestive gland at the end of exposure, which is an indicator of lipid peroxidation and may be explained by antioxidant defense [8]. Again, several biological functions appeared affected upon exposure of products from sacrificial anodes, but this time Al-based ones. But, as mentioned previously, these observations correspond to higher metal concentrations (300 µg/L for Al and 35 µg/L for Zn) and for a longer time of exposure (84 days) than ours.

These different results demonstrate that the Pacific oyster, *Magallana gigas* is sensitive to products emitted by both Zn-and Al-Zn-In-anodes, with some biological effects observed at the highest metal concentrations tested, which are much higher than in our experiments. In the following paragraphs, we discuss the effects of the two types of sacrificial anodes on the different biological functions, as observed with the help of metabolomics, following an untargeted and most sensitive analysis, for nominal concentrations closer to those observed in port conditions.

4.4. Ecotoxicological Effects of Zn- and Al-Zn-In- Anodes on Marine Organisms Assessed by Metabolomics in the Present Study

As mentioned above, the quantities of Zn^{2+} ions to which oysters are actually exposed are higher in the case of Zn-anodes than the total quantity of ions coming from Al-Zn-In anodes. Moreover, there even could be a higher level of exposure to Zn^{2+} ions than to $Al(OH)_4^-$ ions, when using Al-Zn-In anodes. This explains why we found many more metabolites impacted by Zn-anode exposure than by Al-Zn-In: 119 and 124 ions from mass spectrometry analysis for positive and negative modes respectively, showed a significant difference between the reference samples and the samples exposed to Zn-anode, whereas only 63 showed a significant difference between the reference samples and the samples exposed to Al-Zn-In anode. The latest comparison was analyzed in negative mode only, as the two groups could not be clearly separated in positive mode. This also explains why the two metabolites identified as being modulated by Al-Zn-In anode exposure are also among the 16 metabolites modulated by Zn-anode. Thus, it could be that the effects observed in the presence of the Al-Zn-In alloy anodes are probably mainly due to Zn^{2+} ions. An additional argument in favor of this hypothesis is that, among the 61 remaining ions, showing a significant difference between reference and A-Zn-In anode exposed oysters, 31 were also present in the list of ions showing a significant difference between the reference and the Zn-anode exposed samples, but they could not be identified. Further, as illustrated by the low number of identified ions, identification of metabolites remains a challenging task, particularly with not well characterized species such as *Magallana gigas.*

Below we discuss the potential effects of the modulation of the identified metabolites on several biological functions in which they are involved.

4.4.1. Energy Metabolism

Among the metabolites that are impacted by both Zn- and Al-Zn-In anodes, we found the down-regulation of L-phenylalanine. We cannot exclude that this decrease was due to a disturbance of the feeding caused by the induced stress. Nevertheless, it can also be speculated that it may be an indirect effect of energy and lipids metabolism alterations induced by anodes degradation products exposure. Indeed, the exposure to Zn^{2+} or Al^{3+} may lead to an overdemand of energy due to the need to develop protective mechanisms for the cells, such as overproduction of metallothioneins, glutathione, molecular chaperones, antioxidants pathways [31–33]. Furthermore, osmoregulation phenomena, that are overstressed in the presence of metal contaminants, are energetically costly processes and the maintenance of ion gradients is one of the most ATP-consuming processes [34]. L-phenylalanine is an amino acid being both glucogenic and ketogenic and it can be consumed under energy deficient conditions in aquatic invertebrates, in the place of carbohydrates or lipids, which are used in normal

 doi:10.20944/preprints202306.0368.v1

circumstances [34]. Moreover, mitochondrial efficiency and coupling were shown to be reduced and proton leak elevated after exposure to toxic metals such as cadmium, copper, zinc and mercury in marine organisms [34]. In the same way, Meng et al. observed that Zn affected the tricarboxylic acid cycle by influencing the expressions of Fe-containing proteins and disrupted the electron transport chain by inhibiting complex I–IV related protein expressions. This was noted in oysters after 9 days of exposure with nominal Zn concentration of 30 µg/L and analysis of gills by proteomics [35]. More recently, we found a decrease in L-phenylalanine in scallops exposed to Zn^{2+} (150 µg/L), after metabolomic analysis of their gills [18].

Concerning the up modulation of glycerophosphorylcholine observed in our study upon Zn-anode exposition, this could also be linked to energy metabolism disturbances. This compound is a precursor of phosphocholine, as it can be converted into choline and glycerol 3-phosphate by glycerophosphocholine phosphodiesterase and then ATP and choline are converted into phosphocholine and ADP by choline kinase [36]. Recently, Ramirez et al. observed also an up-modulation of glycerophosphocholine in Mediterranean mussels (*Mytilus galloprovincialis*) exposed to a 10 µg/L nominal concentration of the antidepressant venlafaxine and interpreted it as an overdemand in phosphocholine following an inhibition in the conversion of choline and ATP into phosphocholine and ADP [37].

4.4.2. Osmoregulation

Down-modulation of L-phenylalanine observed in both Zn- and Al-Zn-In anodes exposed oysters may also be related to osmoregulation phenomena. Indeed, L-phenylalanine is a precursor of catecholamines, and its lowered level can lead to a decrease in dopamine. The latter molecule is, along with serotonin, a neurotransmitter involved in the modulation of Na^+ and K^+ transport in crustacean gills [38] and in the lateral cilia of bivalve gills [39]. The down-modulation of L-phenylalanine and consequently dopamine could therefore have an impact on osmoregulation in gill cells of oysters exposed to both types of anodes. A similar relationship between the decrease of L-phenylalanine and osmoregulation has been suggested previously [18,40], after 48h-exposure to zinc, respectively $ZnCl_2$ (20, 50, 100 and 150 µg/L) for the clam *Ruditapes decussatus* and Zn^{2+} (150 µg/L) for the variegated scallop (*Mimachlamys varia*). In the first case, the decrease in phenylalanine was associated with a significant increase in the production of organic osmolytes (hypotaurine and homarine) and a decrease in the free amino acid content.

Modulations of proline, proline betaine, betaine and trigonelline in Zn-anode exposed oysters are also related to osmoregulation [41–43]. These molecules affect the ionic strength of the cytosol and thereby maintain osmotic pressure within the cell. Proline was identified as one of the main osmolytes in oyster *Crassostrea virginica* and more generally free amino acids, and among them proline, predominantly contribute to the intracellular pool of osmolytes in all the molluscan species investigated [42]. Proline betaine was identified in bacteria *Staphylococcus aureus* as a highly effective osmoprotectant [41] and as an increasing metabolite in diatoms in response to long term salinity [44]. Betaine and trigonelline are known as organic osmolytes in marine bivalves. Betaine was found to increase in oysters *Crassostrea hongkongensis* after 6-months exposure to metal pollution with a dose-response effect [45] and on the contrary decreased in male oysters *Crassostrea hongkongensis* following *Vibrio harveyi* infection [46]. In female oysters it was rather trigonelline which was found to decrease following *Vibrio harveyi* infection [46]. Trigonelline was also found to vary in *Mytilus galloprovincialis* before and after immune stimulation with *Vibrio splendidus* [47]. In the present study, we observed a down-regulation of betaine in oyster gills after 16 days-exposure to Zn-anode. In study performed in metal polluted estuaries in Southern China, in which Cu and Zn were the major contaminants, Jiu et al. observed also a decrease of betaine in oyster *Crassostrea hongkongensis* gills, in animals exposed to pollution compared to oyster gills from a clean site. This was interpreted as a disturbance of osmotic regulation in gills induced by metals [48]. So, it seems that these organic osmolytes can vary up or down, depending on the different conditions under which the different stressors are applied, also in combination also with other different environmental factors.

 doi:10.20944/preprints202306.0368.v1

The increase in glycerophosphorylcholine upon exposure to Zn-anode could also be attributed to an osmoregulatory mechanism if we refer to the role played by this molecule in humans Indeed, glycerophosphorylcholine is one of the four majors organic osmolytes in renal medullary cells, changing their intracellular osmolyte concentration in parallel with extracellular tonicity during cellular osmoadaptation. Kidneys (especially medullar cells), respond to hypertonic stress by accumulating the organic osmolytes glycerophosphorylcholine, betaine, myo-inositol, sorbitol and free amino acids. Glycerophosphorylcholine is formed in the breakdown of phosphatidylcholine [49].

L-carnitine, which is down-modulated in our study in the presence of Zn-anode, has also been described as an organic osmolyte in bacteria and archaea [50].

Finally, a molecule identified as an eicosanoid was up-regulated in both Zn- and Al-Zn-In anodes exposed oyster gills and this molecule may also have a role in osmoregulation. Eicosanoids correspond to a group of molecules including prostaglandins and related oxygenated metabolites of certain C20 polyunsaturated fatty acids. In addition to many other roles, they are involved in salt and water transport in epithelial tissues in bivalves, leading to release of osmotically active species and restoration of normal cell volume [51,52]. In a study about the influence of salinity on the metabolism of the Pacific oyster *M. gigas*, it was shown that acclimation to salinity involved a major remodeling of membrane fatty acids. Level of arachidonic acid (20:4n-6) varied linearly with salinity, likely reflecting its mobilization for prostaglandin synthesis [52].

4.4.4. Oxidative Stress

Metal pollutants can disrupt mitochondrial function in intertidal bivalves [53] and mitochondria are one of the main sources of ROS, due to electron leakage in respiration [54]. This hypothesis is reinforced by the fact that a decrease in carnitine is simultaneously observed, and that this metabolite was proposed to be a marker of mitochondrial activity after a (^{1}H NMR)-based metabolomic analysis to *Crassostrea virginica*, investigating the differences in the metabolic profile of different organ groups [42].

The decrease in carnitine observed here may also be related to its consumption to play its antioxydant role. The antioxidant defense system is mainly composed of three enzymes: glutathione peroxidase, catalase, and superoxide dismutase. L-carnitine can protect these enzymes from further peroxidative damage [55]. The role of carnitine as antioxidant against lipid peroxidation and against deleterious effects of ROS has already been mentioned in a study of the adverse effects of wastewater effluent on damselfly larvae (*Coenagrion hastulatum*), a common aquatic invertebrate species [56].

4.4.5. Lipid Metabolism

L-carnitine was found to be down-modulated in gills of oysters exposed to Zn-anode. The main function of this compound is the transfer of long-chain fatty acids, in the form of acylcarnitine, to mitochondria for subsequent β-oxidation for energy production. In addition to its role in energy production, carnitine conjugation decreases the number of acyl residues attached to coenzyme A (CoA) and plays a key role in maintaining the homeostasis of the mitochondrial acyl-CoA/CoA ratio [57]. Therefore, the L-carnitine decrease in presence of zinc may be related with both abnormal fatty acid metabolism and mitochondrial dysfunction. In this sense, as we already mentioned above, Tikunov proposed that carnitine may be a useful marker of mitochondrial activity, after metabolomic analysis of *Crassostrea virginica* different organ groups [42].

The process of long-chain fatty acids transport, known as carnitine shuttle pathway, was found to be disturbed in several studies about invertebrates exposed to pollutants, with most of the time changes in acylcarnitine profiles, rather than decrease in carnitine, as is the case in the present study. For example, diclofenac was found to affect the carnitine shuttle pathways in *Hyalella azteca*, a freshwater invertebrate, at environmentally relevant concentrations, showing the decrease of three different acylcarnitine [58]. In another recent study, three different acylcarnitine were up-regulated in damselfly larvae (*Coenagrion hastulatum*), after wastewater effluent exposure [56]. We observed changes in acylcarnitine profiles when scallops were exposed to different stressors in laboratory conditions: an increase of seven different acylcarnitine metabolites at the end of the two hours

 doi:10.20944/preprints202306.0368.v1

emersion periods [22], a down-regulation of three after 48 h-exposure to a nominal zinc concentration of 150 µg/L [18] and up-regulation of one under 48h-exposure to a copper concentration of 82 µg/L) [59]. All these observations concern situations found in the environment, and it therefore seems that the carnitine shuttle pathway is frequently impacted by various stressors: pharmaceutical residues, metallic pollutants or anoxia.

It should be added that carnitine also functions as a scavenger, by binding acyl residues deriving from the intermediary metabolism of amino acids and helping in their elimination. This mechanism is essential in binding/removing abnormal organic acids and is likely to cause carnitine deficiency [57].

3-Dehydrocarnitine, an intermediate in carnitine degradation, was also found to decrease in the present study, in gills of Zn-anode exposed oysters. This metabolite was found to be significantly dysregulated in a study about the possible adverse effects of fadrozole, a molecule used in breast-cancer medication, on the adult freshwater mussel *Lampsilis fasciola* [60].

Dodecanedioic acid was found to be down-modulated in Zn-anode exposed oysters. This metabolite is a dicarboxylic acid, which can be rapidly oxidized in the peroxisomes and then transferred to the mitochondria for further degradation. It might be derived from long monocarboxylic acids through an initial ω-oxidation followed by β-oxidation [61]. Thus, the observed decrease of dodecanedioic acid could indicate peroxisomal dysfunction.

4.4.6. Nucleotide and Nucleoside Metabolism

Both adenine and adenosine were found to decrease in the presence of Zn-anode. Adenine, a purine derivative, forms adenosine, a nucleoside, when attached to ribose and deoxyadenosine when attached to deoxyribose. Adenine is therefore one of four nitrogenous bases at the origin of nucleic acids (both RNA and DNA) synthesis. Adenosine can be bonded with from one to three phosphoric acid units, yielding the energy carriers adenosine mono-, di-, and triphosphate (AMP, ADP and ATP). Adenosine also plays a role in signal transduction as cyclic adenosine monophosphate (cAMP). Guanosine was found to be up-modulated in presence of Zn-anode. This purine derivative is also involved in various biochemical processes including the synthesis of nucleic acids such as RNA and intracellular signal transduction. This last role is played by cyclic guanosine monophosphate (cGMP), which is one of the phosphorylated forms of guanosine, with guanosine monophosphate (GMP), guanosine diphosphate (GDP), and guanosine triphosphate (GTP).

Adenine, adenosine and guanosine are therefore essential for life and their metabolic relationships with many metabolic pathways are strong, which makes it difficult to interpret their modulation. It may correspond to restriction of substrates involved in DNA and RNA turnover and repair, overdemand of energy carrier to develop detoxification processes, inhibition of key enzymes involved in purine and synthesis or altered phosphagen metabolism. Impact of pollution on nucleotide metabolism of marine mollusk or fish has often been mentioned [59,62–64].

We already observed a disordered nucleotide metabolism in scallops exposed to Zn, manifesting by a lower level of xanthine [18]. Indeed, in the catabolism of purine nucleotides, adenosine monophosphate (AMP) and GMP both lead to xanthine.

In a study of the effect of pharmaceutical active compounds on *Danio rerio* fish antibiotic-exposed for 72 h, it was found that the main affected metabolic pathway was related to purine metabolism, especially guanosine [65]. The authors mention that this compound has been shown to be involved in protecting neurons against excitotoxic damage in vertebrates, but its role in invertebrates has not been fully explored yet.

4.4.7. Amino Acids Metabolism

Xanthurenic acid, which is a metabolite from tryptophan catabolism, was up-regulated in gills of Zn-anode exposed oysters, indicating that the tryptophan metabolism was disturbed. Tryptophan is not only essential for protein biosynthesis but also serves as a precursor to serotonin, a main actor in the neuroendocrine-immune regulation in marine bivalves [66].

 doi:10.20944/preprints202306.0368.v1

4.4.8. Defense or Signaling Pathways

Turicine (cis-4-Hydroxy-D-proline betaine), also known as combretin A, was found to decrease in gills of oysters exposed to Zn-anode. This proline derivative is a secondary metabolite. As such, it may serve as defense or signalling molecule, or it may be simply a molecule that arises from the degradation of other secondary metabolites.

Eicosanoids already mentioned for their role in osmoregulation have also been shown to be important cellular signaling molecules related to inflammation and immune regulation in invertebrates [67]. A molecule identified as an eicosanoid was up- regulated in both Zn- and Al-Zn-In anodes exposed oysters.

5. Conclusions

Our study demonstrates the early effects of exposure of oysters to the degradation products of both types of sacrificial anodes used to protect marine metal structures from corrosion: Zn- and Al-Zn-In-anodes. These effects were however observed with released Al and In concentrations 25 times higher than those expected in the seaport used as reference (La Rochelle commercial seaport, Atlantic coast, France), and 42 times higher in the case of Zn.

These effects are observable mainly for oysters exposed to the Zn-anode, when the digestive gland has not yet accumulated zinc. For this first type of anode, the main dissolved degradation product is Zn^{2+}. For Al-Zn-In anodes, our chemical modelling study indicates that the main dissolved species among degradation products is $Al(OH)_4^-$, but even though Al is the overwhelmingly majority constituent and Zn a very minority constituent of anodes, there even could be a higher level of exposure to Zn^{2+} ions than to $Al(OH)_4^-$ ions, due to solubility properties of both elements. Thus, the effects observed in the presence of the Al-Zn-In alloy anodes could mainly be due to Zn^{2+} ions, hence the interest in limiting the percentage of zinc in this type of alloy to a minimum. However, the effects on oyster metabolism seem to be less pronounced than for the Zn-anode, which is an important finding of this study.

No detectable effect attributable to indium was observed in our experimental conditions. It must be recalled that this element is present as traces (~0.02 wt.%) in Al-Zn-In anodes.

Our experimentation has been performed under optimal conditions of temperature, salinity and food availability for exposed oysters. It would be interesting to evaluate the energetic cost of the metabolomic changes observed, especially under more constraining environmental conditions, and for a longer exposure time.

As mentioned above, only a few ions were identified, mainly due to the low characterization of the studied species. Even if mass spectrometry is a powerful and sensitive tool, analysts generally face difficulties concerning identification, especially in metabolomics. Here, to improve the identification rate, we queried all databases offered in the Sirius software. Unfortunately, many ions remain unidentified, affecting our reading of metal exposure consequences on oysters. So, structure databases need to be completed to make metabolites identification easier.

One of the strong points of this study was to combine chemical modelling of the degradation products of both sacrificial Zn- and Al-Zn-In anodes, with a metabolomic approach to identify the effects of these anodes on the metabolism of the oyster, in an untargeted way. We in fact studied the exposure of a cocktail of products, soluble or not, on the oyster and not the effect of a metal in a single cationic form.

Author Contributions: Conceptualization, N.I., D.F., R.S., P.R. and M.G.; methodology, N.I., D.F.,P.-E.B., R.S., P.R. and M.G.; software, N.I., P.O., P.-E.B. and M. G.; validation, N.I., D.F.,P.-E.B., R.S., P.R. and M.G.; formal analysis, N.I., D.F.,P.-E.B., R.S., P.R. and M.G.; investigation, N.I., D.F.,P.-E.B., P.R. and M.G.; data curation, P.O., P.-E.B., L.M. and M.G.; writing—original draft preparation, N.I., D.F.,P.-E.B., R.S., P.R. and M.G.; writing—review and editing, N.I., D.F.,P.-E.B., P.O., R.S., P.R. and M.G.; supervision, P.R. and M.G.; project administration, P.R. and M.G.; funding acquisition, P.R. All authors have read and agreed to the published version of the manuscript.

Funding: This research was funded by PORT ATLANTIQUE LA ROCHELLE, Research Program MA5 -Port Horizon 2025.

Institutional Review Board Statement: Not applicable.

Informed Consent Statement: Not applicable.

Data Availability Statement: Data is contained within the article.

Acknowledgments: We gratefully thank Valérie Huet for technical assistance for metabolites extraction from oyster gills, Emmanuel Dubillot for technical assistance during animal experiments, Carine Churlaud and Maud Brault Favrou for analysis performed in the "Plateforme Analyses Elémentaires". These four engineers or assistant engineers are from laboratory "Littoral Environnement et Sociétés" (LIENSs), UMR 7266, CNRS-La Rochelle Université, 2 rue Olympe de Gouges, F-17042 La Rochelle Cedex 01, France). We also thank B. Simon-Bouhet for his help to make graph on R-Studio and Adèle Gourcerol who helped us for dissection phase during her internship.

Conflicts of Interest: The authors declare no conflict of interest. The funders had no role in the design of the study; in the collection, analyses, or interpretation of data; in the writing of the manuscript, or in the decision to publish the results.

References

1. Davy, H. On the corrosion of copper sheeting by sea water, and on methods of preventing this effect; and on their application to ships of war and other ships. *Phil. Trans. Royal Soc. London* **1824**, *114*, 151-158.
2. Lemieux, E.; Hartt, W.H.; Lucas, K.E. A critical review of Al anode activation and dissolution mechanisms and performance. Paper NACE-01509, CORROSION 2001 conference, Houston, Texas, USA, 11-16 March 2001.
3. Muñoz, A.G.; Saidman, S.B.; Bessone, J.B. Corrosion of an Al–Zn–In alloy in chloride media. *Corros. Sci.* **2002**, *44*, 2171-2182.
4. Ma, J.; Wen, J.; Zhai, W.; Li, Q. In situ corrosion of Al-Zn-In-Mg-Ti-Ce sacrificial anode alloy. *Mater. Charac.* **2012**, *65*, 86-92.
5. Caplat, C., Oral, R., Mahaut, M.-L., Mao, A., Barillier, D., Guida, M., Della Rocca, C., Pagano, G. Comparative toxicities of aluminum and zinc from sacrificial anodes or from sulfate salt in sea urchin embryos and sperm. *Ecotoxicol. Environ. Saf.* **2010**, 73, 1138–1143.
6. Muttin, E., Caplat, C.,Latire, T., Mottier, A., Mahaut, M.-P., Costil, K., Barillier, D., Lebel, J.-M., Serpentini, A. Effect of zinc sacrificial anode degradation on the defence system of the Pacific oyster, *Crassostrea gigas*: Chronic and acute exposures. *Marine Pollution Bulletin* **2012**, 64, 1911-1920.
7. Barbarin, M., Turquois, C., Dubillot, E., Huet, V., Churlaud, C., Muttin, F., Thomas, H. First quantitative biomonitoring study of two ports (marina, commerce) in French littoral area: Evaluation of metals released into the marine environment and resulting from galvanic anodes. *Sci. Total Environ.* **2023**, 857, 159244.
8. Levallois, A., Caplat, C., Basuyaux, O., Lebel, J.-M., Laisney, A., Costil, K., Serpentini, A. Effects of chronic exposure of metals released from the dissolution of an aluminium galvanic anode on the Pacific oyster *Crassostrea gigas*. *Aquatic Toxicology* **2022**, 249, 1062232022.
9. Breitwieser, M.; Vigneau, E.; Viricel, A.; Becquet, V.; Lacroix, C.; Erb, M.; Huet, V.; Churlaud, C.; Le Floch, S.; Guillot, B., Graber, M., Thomas, H. What is the relationship between the bioaccumulation of chemical contaminants in the variegated scallop *Mimachlamys varia* and its health status? A study carried out on the French Atlantic coast using the Path ComDim model. *Sci. Total Environ.* **2018**, 640, 662–670.
10. Gibson, G. Behavior of Al-Zn-In anodes at elevated temperature. Paper NACE-10369, CORROSION 2010 conference, San Antonio, Texas, USA, 14-18 March 2010.
11. Parkhurst, D.L.; Appelo, C.A.J. User's guide to PHREEQC (Version 2) - A computer program for speciation, batch-reaction, one-dimensional transport, and inverse geochemical calculations: U.S. Geological Survey. *Water-Resour. Investig. Rep.* **1999**, *312*, 99–4259.
12. Allison, J.D.; Brown, D.S.; Novo-Gradac, K.J. MINTEQA2/PRODEFA2—A Geochemical Assessment Model for Environmental Systems—Version 3.0 User's Manual; Environmental Research Laboratory, Office of Research and Development U.S. Environmental Protection Agency: Athens, GA, USA, 1990.
13. U.S. Environmental Protection Agency. MINTEQA2/PRODEFA2, A Geochemical Assessment Model for Environmental Systems—User Manual Supplement for Version 4.0; National Exposure Research Laboratory, Ecosystems Research Division: Athens, GA, USA, 1998.
14. ASTM D1141-98(2021), Standard Practice for Preparation of Substitute Ocean Water. ASTM International: West Conshohocken, PA, USA, 2021.
15. Soto, M., Ireland, M.P., Marigómez, I. The contribution of metal/shell-weight index in target-tissues to metal body burden in sentinel marine molluscs *Littorina littorea*. *Sci Total Environ.* **1997**, 198, 135–147.

16. Miramand, P., Bustamante, P., Bentley, D., Kouéta, N. Variation of heavy metal concentrations (Ag, Cd, Co, Cu, Fe, Pb, V, and Zn) during the life cycle of the common cuttlefish *Sepia officinalis*. *Sci. Total Environ.* **2006**, 361, 132–143.
17. Metian, M., Warnau, M., Oberhansli, F., Teyssie, J.L., Bustamante, P. Interspecific comparison of Cd bioaccumulation in European Pectinidae (*Chlamys varia* and *Pecten maximus*). *J. Exp. Mar. Biol. Ecol.* **2007**, 353, 58–67.
18. Ory, P., Hamani, V., Bodet, P.E., Murillo, L., Graber, M. The variegated scallop, *Mimachlamys varia*, undergoes alterations in several of its metabolic pathways under short-term zinc exposure. *Comp. Biochem. Physiol. Part D Genom. Proteom.* **2021**, 37, 100779.
19. Ravera, O. Monitoring of the aquatic environment by species accumulator of pollutants: A review. *J. Limnol.* **2001**, 60, 63–78.
20. Trevisan, R.; Mello, D.F.; Delapedra, G.; Silva, D.G.H.; Arl, M.; Danielli, N.M.; Metian, M.; Almeida, E.A.; Dafre, A.L. Gills as a glutathione-dependent metabolic barrier in Pacific oysters *Crassostrea gigas*: Absorption, metabolism and excretion of a model electrophile. *Aquat. Toxicol.* **2016**, 173, 105–119.
21. Mondeguer, F.; Abadie, E.; Herve, F.; Bardouil, M.; Sechet, V.; Raimbault, V.; Berteaux, T.; Zendong, S.Z.; Palvadeau, H.; Amzil, Z.; et al. Pinnatoxines en lien avec l'espèce *Vulcanodinium rugosum* (II). **2015**. Available online: http://archimer.ifremer.fr/doc/00285/39635/ (accessed on 31 March 2023).
22. Ory, P.; Bonnet, A.; Mondeguer, F.; Breitwieser, M.; Dubillot, E.; Graber, M. Metabolomics based on UHPLC-QToF- and APGCQToF-MS reveals metabolic pathways reprogramming in response to tidal cycles in the sub-littoral species Mimachlamys varia exposed to aerial emergence. Comp. Biochem. Physiol. Part D Genom. Proteom. 2019, 29, 74–85.
23. Van Der Kloet, F.M.; Bobeldijk, I.; Verheij, E.R.; Jellema, R.H. Analytical error reduction using single point calibration for accurate and precise metabolomic phenotyping. *J. Proteome Res.* **2009**, *8*, 5132–5141.
24. Dührkop, K., Fleischauer, M., Ludwig, M., Aksenov, A.A., Melnik, A.V., Meusel, M., Dorrestein, P.C., Rousu, J., Böcker, S. SIRIUS 4: a rapid tool for turning tandem mass spectra into metabolite structure information. *Nat. Methods* **2019**, 16, 299-302.
25. Schymanski, E.L.; Jeon, J.; Gulde, R.; Fenner, K.; Ruff, M.; Singer, H.P.; Hollender, J. Identifying small molecules via high resolution mass spectrometry: Communicating confidence. *Environ. Sci. Technol.* **2014**, 48, 2097–2098.
26. Gensemer, R.W., Playle, R.C. The bioavailability and toxicity of aluminum in aquatic environments. *Crit. Rev. Environ. Sci. Technol.* **1999**, *29*, 315-450.
27. Caplat, C., Mottin, E., Lebel, J.-M., Serpentini, A., Barillier, D., Mahaut M.-L. Impact of a Sacrificial Anode as Assessed by Zinc Accumulation in Different Organs of the Oyster *Crassostrea gigas*: Results from Long- and Short-Term Laboratory Tests. *Arch Environ Contam Toxicol* **2012,** 62, 638–649.
28. Mao, A., Mahaut, M.-L., Pineau, S., Barillier, D. Assessment of sacrificial anode impact by aluminum accumulation in mussel Mytilus edulis: A large-scale laboratory test. *Marine Pollution Bulletin* **2011,** 62, 2707–2713.
29. Kirchgeorg, T., Weinberg, I., Hörnig, M., Baier, R., Schmid, M.J., Brockmeyer, B. Emissions from corrosion protection systems of offshore wind farms: Evaluation of the potential impact on the marine environment. *Marine Pollution Bulletin* **2018,** 136, 257–268.
30. Yang, J.-L. Comparative acute toxicity of gallium(III), antimony(III), indium(III), cadmium(II), and copper (II) on freshwater swamp shrimp (*Macrobrachium nipponense*). *Biological Research* **2014**, 47, 13.
31. Cherkasov, A.S., Effects of acclimation temperature and cadmium exposure on cellular energy budgets in the marine mollusk *Crassostrea virginica*: linking cellular and mitochondrial responses. J. Exp. Biol. **2006**, 209, 1274–1284.
32. Ivanina, A.V., Cherkasov, A.S., Sokolova, I.M. Effects of cadmium on cellular protein and glutathione synthesis and expression of stress proteins in eastern oysters, *Crassostrea virginica* Gmelin. J. Exp. Biol. **2008**, 211, 577–586.
33. Sokolova, I.M., Lannig, G. Interactive effects of metal pollution and temperature on metabolism in aquatic ectotherms: implications of global climate change. *Clim. Res.* **2008**, 37, 181–201.
34. Sokolova, I.M., Frederich, M., Bagwe, R., Lannig, G., Sukhotin, A.A. Energy homeostasis as an integrative tool for assessing limits of environmental stress tolerance in aquatic invertebrates. *Mar. Environ. Res.* **2012**, 79, 1–15.
35. Meng, J., Wang, W.-X., Li, L., Zhang, G. Respiration disruption and detoxification at the protein expression levels in the Pacific oyster (*Crassostrea gigas*) under zinc exposure. *Aquat. Toxicol.* **2017**, 191, 34–41.
36. Liu, X., Sun, H., Wang, Y., Ma, M., Zhang, Y. Gender-specific metabolic responses in hepatopancreas of mussel *Mytilus galloprovincialis* challenged by *Vibrio harveyi.* **2014**, *Fish & Shellfish Immunology* 40, 407-413.
37. Ramirez, G., Gomez, E., Dumas, T., Rosain, D., Mathieu, O., Fenet, H., Courant, F. Early Biological Modulations Resulting from 1-Week Venlafaxine Exposure of Marine Mussels *Mytilus galloprovincialis* Determined by a Metabolomic Approach. **2022**, *Metabolites* 12, 197.

38. Mo, J.L., Devos, P., Trausch, G. Dopamine as a modulator of ionic transport and Na+/K+-ATPase activity in the gills of the chinese crab *Eriocheir sinensis*. **1998**, *J. Crustac.Biol.* 18, 442–448.
39. Carroll, M.A., Catapane, E.J. The nervous system controls of lateral ciliary activity of the gill of the bivalve mollusc, *Crassostrea virginica*. **2007**, *Comp. Biochem. Physiol. A. Mol. Integr. Physiol.* 148, 445–450.
40. Aru, V., Sarais, G., Savorani, F., Engelsen, S.B., Cesare Marincola, F. Metabolic responses of clams, *Ruditapes decussatus* and *Ruditapes philippinarum*, to short-term exposure to lead and zinc. **2016**, *Mar. Pollut. Bull.* 107, 292–299.
41. Amin, U. S., Lash, T. D., Wilkinson B. J. Proline betaine is a highly effective osmoprotectant for *Staphylococcus aureus*. **1995**, *Arch Microbiol* 163, 138-142.
42. Tikunov, A.P., Johnson, C.B., Lee, H., Stoskopf, M.K., Macdonald, J.M. Metabolomic Investigations of American Oysters Using 1H-NMR Spectroscopy. **2010**, *Mar. Drugs* 8, 2578-2596.
43. Zhou, C., Song, H., Feng, J., Hu, Z., Yang, M.J., Shi, P., Guo, Y.J., Li, H.Z., Zhang, T. Metabolomics and biochemical assays reveal the metabolic responses to hypo-salinity stress and osmoregulatory role of cAMP-PKA pathway in *Mercenaria mercenaria*. **2022**, *Computational and structural Biotechnology Journal* 120, 4110-4121.
44. Nikitashina, V., Stettin, D., Pohnert, G. Metabolic adaptation of diatoms to hypersalinity. **2022**, *Phytochemistry* 201, 113267.
45. Cao, C., Wang, W.-X. Bioaccumulation and metabolomics responses in oysters *Crassostrea hongkongensis* impacted by different levels of metal pollution. **2016**, *Environmental Pollution* 216, 156-165.
46. Ma, L., Lu, J., Yao, T., Ye, L., Wang, J. Gender-Specific Metabolic Responses of *Crassostrea hongkongensis* to Infection with *Vibrio harveyi* and Lipopolysaccharide. **2021**, *antioxidants* 11, 1178.
47. Frizzo, R., Bortoletto, E., Riello, T., Leanza, L., Schievano, E., Venier, P., Mammi, S. NMR Metabolite Profiles of the Bivalve Mollusc *Mytilus galloprovincialis* Before and After Immune Stimulation With *Vibrio splendidus*. **2021**, *Frontiers in Molecular Biosciences* 8, 686770.
48. Ji, C., Wang, Q., Wua, H., Tan, Q., Wang, W.-X. A metabolomic investigation of the effects of metal pollution in oysters *Crassostrea hongkongensis*. **2015**, *Marine Pollution Bulletin* 90, 317–322.
49. Gallazzini, M., Burg M. B. What's New About Osmotic Regulation of Glycerophosphocholine. **2009**, *Physiology* 24, 204-266.
50. Burg, M. B., Ferraris, J.D. Intracellular Organic Osmolytes: Function and Regulation. **2008**, *J. Biol. Chem.* 283, 7309-7313.
51. Stanley-Samuelson, D.W. The Biological Significance of Prostaglandins and Related Eicosanoids in Invertebrates. **1994**, *Amer. Zool.* 34, 589-598.
52. Fuhrman, M., Delisle, L., Petton, B., Corporeau, C., Pernet, F. Metabolism of the Pacific oyster, *Crassostrea gigas*, is influenced by salinity and modulates survival to the Ostreid herpes virus OsHV-1. **2018**, *Biology Open* 7.
53. Ivanina, A.V., Sokolova, I.M. Interactive effects of pH and metals on mitochondrial functions of intertidal bivalves *Crassostrea virginica* and *Mercenaria mercenaria.* **2013**, *Aquatic Toxicology* 144– 145, 303– 309.
54. Handy, D.E., Loscalzo, J. Redox Regulation of Mitochondrial Function. **2012**, *Antioxidants and Redox Signaling* 16, 1323-1367.
55. Gülçin, I. Antioxidant and antiradical activities of l-carnitine. **2006**, *Life Sciences* 78, 803-811.
56. Späth, J., Fick, J., McCallum, E., Cerveny, D., Nording, M.L., Brodin, T. Wastewater effluent affects behaviour and metabolomic endpoints in damselfly larvae. **2022**, *Scientific Reports* 12, 6830.
57. Longo, N., Frigeni, M., Pasquali, M. Carnitine transport and fatty acid oxidation. **2016**, *Biochim. Biophys. Acta* 1863, 2422-2435.
58. Fu, Q., Scheidegger, A., Laczko, E., Hollender, J. Metabolomic Profiling and Toxicokinetics Modeling to Assess the Effects of the Pharmaceutical Diclofenac in the Aquatic Invertebrate *Hyalella azteca.* **2021**, *Environ. Sci. Technol.* 55, 7920–7929.
59. Hamani, V., Ory,P., Bodet, P.-E., Murillo, L., Graber, M. Untargeted Metabolomics Reveals a Complex Impact on Different Metabolic Pathways in Scallop *Mimachlamys varia* (Linnaeus, 1758) after Short-Term Exposure to Copper at Environmental Dose. **2021**, *Metabolites* 11, 862.
60. Léonard, J.A., Cope, W.G., Barnhart, M.C., Bringolf, R.B. Metabolomic, behavioral, and reproductive effects of the aromatase inhibitor fadrozole hydrochloride on the unionid mussel *Lampsilis fasciola*. **2014**, *General and Comparative Endocrinology* 206, 213-226.
61. Ferdinandusse, S., Denis, S., van Roermund, C.W.T., Wanders, R.J.A., Dacremont, G. Identification of the peroxisomal β-oxidation enzymes involved in the degradation of long-chain dicarboxylic acids. **2004**, *Journal of Lipid Research* 45, 1104-1111.
62. Watanabe, M., Meyer, K.A., Jackson, T.M., Schock, T.B., Johnson, W.E., Bearden, D.W. Application of NMR-based metabolomics for environmental assessment in the Great Lakes using zebra mussel (*Dreissena polymorpha*). **2015**, Metabolomics 11, 1302-1315.

63. Cappello, T., Maisano, M., Mauceri, A., Fasulo, S. 1 H NMR-based metabolomics investigation on the effects of petrochemical contamination in posterior adductor muscles of caged mussel *Mytilus galloprovincialis*. **2017**, *Ecotoxicol. Environ. Saf.* 142, 417–422.
64. Dumas, T., Bonnefille, B., Gomez, E., Boccard, J., Ariza Castro, N., Fenet, H., Courant, F. Metabolomics approach reveals disruption of metabolic pathways in the marine bivalve *Mytilus galloprovincialis* exposed to a WWTP effluent extract. **2020,** *Science of the Total Environment* 712, 136551.
65. De Sotto, R.B., Medriano, C.D., Cho, Y., Kim, H., Chung, I;-Y., Seok, K.-S., Hong, S.W., Park, Y., Kim, S. Sub-lethal pharmaceutical hazard tracking in adult zebrafish using untargeted LC–MS environmental metabolomics. **2017**, *Journal of Hazardous Materials* 339, 63–72.
66. Canesi, L., Miglioli, A., Balbi, T., Fabbri, E. Physiological Roles of Serotonin in Bivalves: Possible Interference by Environmental Chemicals Resulting in Neuroendocrine Disruption. **2022**, *Frontiers in Endocrinology* 13, 792589.
67. Monmai, C., Go, S.H., Shin, I.S., You, S.G., Lee, H., Kang, S.B., Park, W.J. Immune-Enhancement and Anti-Inflammatory Activities of Fatty Acids Extracted from *Halocynthia aurantium* Tunic in RAW264.7 Cells. **2018**, *Mar. Drugs* 16, 309.